Full Paper

Applied Organometallic Chemistry

Received: 7 May 2008 Revised: 18 June 2008 Accepted: 18 June 2008 Published online in Wiley Interscience: 11 August 2008

(www.interscience.com) DOI 10.1002/aoc.1440

Two novel Ag(I) coordination polymers with triazoles derivatives: synthesis, crystal structures and biological activity

Xinli Han, Changxue An and Zhihui Zhang*

Two novel coordination polymers, $[Ag(L_1)(NO_3)]_n$ 1 and $[Ag(L_2)_2(ClO_4)]_n$ 2 [L_1 = 1-(1-benzotriazole-yl-)triazole, L_2 = 1-(4-chloro-pyridazine-yl-)triazole] have been synthesized and characterized. Single-crystal X-ray analyses show that the Ag(I) atom is in a four-coordinated distorted tetrahedron environment, which are linked by the coordinated nitrate group and L_1 into a two-dimensional network in complex 1. While in the complex 2, the Ag(I) is also in a distorted tetrahedron environment consisting of four N atoms to present a one-dimensional infinite chain, the intermolecular $\pi - \pi$ stacking action extends further the repeated units into three-dimensional topological framework. The biological activities of the title compounds have been studied. The results indicate that two ligands exhibit excellent radical-scavenging activities and certain fungicidal activities, and both Ag(I) complexes only have good antibacterial activities. Furthermore, the studies on luminescent properties of the complexes in the solid state indicate that the Ag(I) complexes exhibit weaker fluoresce intensity than that of ligands at room temperature.

Supporting information may be found in the online version of this article.

Keywords: triazole; Ag(I) complex; pyridazine; fungicidal activity; radical-scavenging activity

Introduction

The chemistry of coordination polymers or multi-nuclear metal complexes with organic–inorganic chelating ligands has received much attention because of their potential applications in functional materials, medicines and agriculture chemicals.[1,2] In this area, the design and synthesis of the functional ligand is a good way to realize the applications of the complexes. Triazole and its derivatives are versatile ligands because these compounds not only provide multi-coordinated sites to link more metal centers but also provide excellent $\pi - \pi$ stacking interactions between the rings to generate multi-nuclear complexes or polymers.[3–10] The functional substituted group on triazole ring can decorate the structure of triazole compounds and affect the coordination configuration and functions of the metal complexes as well. Furthermore, the biological activities of the triazole compounds enhance the function of the metal complexes with triazole ligands

Triazole compounds were introduced by Trofimenko in 1967.[11] These compounds unite the coordination geometry of both pyrazoles and imidazoles and exhibit a strong and typical property of action as bridging ligands between two metal ions,[12] such as silver(I) complex with 1,2-bis(1,2,4-triazole-1-yl)methane and copper(II) complex with triazole derivatives have been reported.[13–16]

In order to inspect the relationships of the molecular structures with the properties of metal complexes, herein we report two novel Ag(I) coordination polymers with two triazole derivatives containing benzotriazole and pyridazine functional groups.

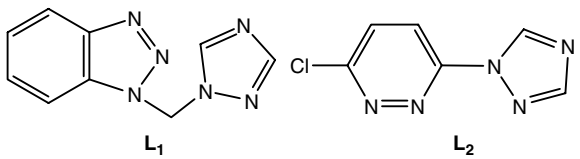

L_1 L_2

Scheme 1. The molecular structures of L_1 and L_2.

Experimental

Materials and general methods

All chemicals were of analytical reagent grade and used as received without further purification. Solvents were purified according to the standard methods prior to use. The L_1 and L_2 ligands were synthesized according to the literature methods[17,18] (Scheme 1).

FT-IR spectra were recorded on a Shimadzu IR-408 infrared spectrophotometer in the 4000–400 cm^{-1} region. Elemental analyses of carbon, hydrogen and nitrogen were carried out with a Perkin-Elmer model 240 analyzer. Electronic spectra were recorded on a Shimadzu-UV-2450 spectrophotometer in the 200–800 nm range. Emission spectra in the solid state were taken on a WGY-10 spectrophotometer at room temperature. ^1H NMR spectra were recorded on a Bruker AC-P300 spectrometer at room temperature in DMSO (d6).

* *Correspondence to: Zhihui Zhang, The Department of Chemistry, Nankai University, Tianjin 300071, People's Republic of China. E-mail: zhangzh67@nankai.edu.cn*

The Department of Chemistry, Nankai University, Tianjin 300071, People's Republic of China

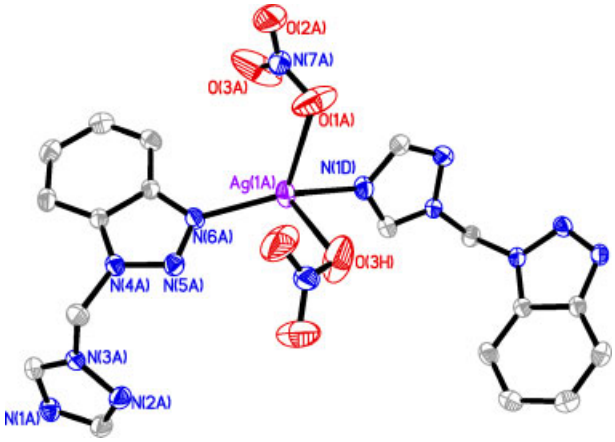

Figure 1. ORTEP view of the complex **1,** and 30% probability for the ellipsoids. Hydrogen atoms are omitted for clarity.

Synthesis of $[Ag(L_1)(NO_3)]_n$, 1

$AgNO_3$ (17.0 mg, 0.1 mmol) was dissolved in water (3 ml) in a test tube. A buffer solution (6 ml) of acetone and water (v/v = 1 : 1) was carefully added to the solution of $AgNO_3$. A solution of L_1 (20.0 mg, 0.1 mmol) in acetone (3 ml) was then added to the buffer layer without disturbing the three layers. Colorless single crystals of **1** suitable for X-ray analysis were obtained after *ca* three weeks. Yield: 25.1 mg, 67.8% (based on Ag). Calcd for $C_9H_8AgN_7O_3$ (%): C, 29.32; H, 2.07; N, 26.51. Found (%): C, 29.21; H, 2.18; N, 26.49. IR (KBr pellets, cm^{-1}): 3095 (s), 3031 (w), 1597 (w), 1525 (m), 1470(m), 1380 (s, NO_3^-), 1320(s),1280 (s), 1227 (s), 1115 (s), 1012 (m), 900 (br), 792 (s), 750 (s), 681 (m), 610 (m). ^{1}H NMR(DMSO): δ = 6.2(-CH_2), 7.3–7.7(ben), 8.1, 9.0 (trizole).

Table 2. Selected bonds lengths (Å) and angles (deg) for **1**

Bonds lengths			
Ag (1)–N (6)	2.181(4)	Ag (1)–O (1)	2.586(5)
Ag (1)–N (1)$^{\#1}$	2.187(4)	N (1)–Ag (1)$^{\#2}$	2.187(4)
Ag (1)–O (3A)	2.630		
Bonds angles			
N(6)–Ag (1)–N (1)$^{\#1}$	153.4(16)	C (2)–N (1)–Ag (1)$^{\#2}$	128.3(3)
N(6)–Ag (1)–O (1)	112.8(2)	C (1)–N (1)–Ag (1)$^{\#2}$	127.8(3)
N (1)$^{\#1}$–Ag (1)–O (1)	90.8(2)		

Symmetry transformations used to generate equivalent atoms: $^{\#1}$ $-x, y-1/2, -z+3/2$; $^{\#2}$ $-x, y+1/2, -z+3/2$.

Synthesis of $[Ag(L_2)_2(ClO_4)]_n$, 2

Complex **2** was prepared using a similar procedure to complex **1**, except L_2 was used instead of L_1, and $AgClO_4$ was used instead of $AgNO_3$. Colorless single crystals of **2** suitable for X-ray analysis were obtained after *ca* two weeks. Yield: 26.1 mg, 45.7% (based on Ag). Calcd for $C_{12}H_8AgCl_3N_{10}O_4$ (%): C, 25.38; H, 1.29; N, 24.71. Found (%): C, 25.26; H, 1.40; N, 24.55. IR (KBr pellets, cm^{-1}): 3452 (br), 3115 (m), 1580 (m), 1525 (s), 1454 (s), 1370 (s), 1299 (s), 1215 (m), 1117 (s), 1089 (s, ClO_4^-), 1031(s), 976 (m), 849 (m), 779 (m), 666 (m). ^{1}H NMR (DMSO) : δ = 8.2, 8.3 (pyridazine), 8.5, 8.8 (trizole).

X-ray crystallography

The single crystals with dimensions 0.30 × 0.20 × 0.20 mm for complex **1** and 0.40 × 0.30 × 0.05 mm for complex **2** were selected and mounted on a Bruker Smart CCD area detector with graphite monochromatized MoKα radiation (λ = 0.71073 Å). All the data were collected at room temperature using the $\omega - 2\theta$

Table 1. Crystal data and structure refinement for **1** and **2**

Complexes	**1**	**2**
Empirical formula	C_9 H_8 Ag N_7 O_3	C_{12} H_8 Ag Cl_3 N_{10} O_4
Formula weight	370.09	570.50
Temperature (K)	293(2)	293(2)
System, space group	Monoclinic, P2(1)/c	Monoclinic, P2/c
a (Å)	7.2114(14)	16.981(3)
b (Å)	17.333(4)	7.6784(15)
c (Å)	9.916(2)	15.656(3)
β (deg)	96.16(3)	106.58(3)
V (Å^3)	1232.3(4)	1956.5(7)
Z	4	4
Crystal size mm	0.30 × 0.20 × 0.20	0.40 × 0.30 × 0.05
D_{calcd} (g cm^{-3})	1.995	1.937
μ (MoKα) (mm^{-1})	1.656	1.485
F (000)	728	1120
2θ range (deg)	3.07–25.01	2.98–25.01
Reflections collected	10 502	16 164
Independant reflections (R_{int})	2168(0.0266)	3437(0.0571)
GOF on F^2	1.099	1.055
Data/restraints/parameters	2168/0/181	3437/0/272
Final R_1 and wR_2 [$I > 2\sigma(I)$]	0.0438, 0.1074	0.0585, 0.1384
R_1 and wR_2 [all data]	0.0481, 0.1101	0.0787, 0.1494
Largest difference peak and hole (e Å^{-3})	0.944 and −0.731	0.887 and −0.891

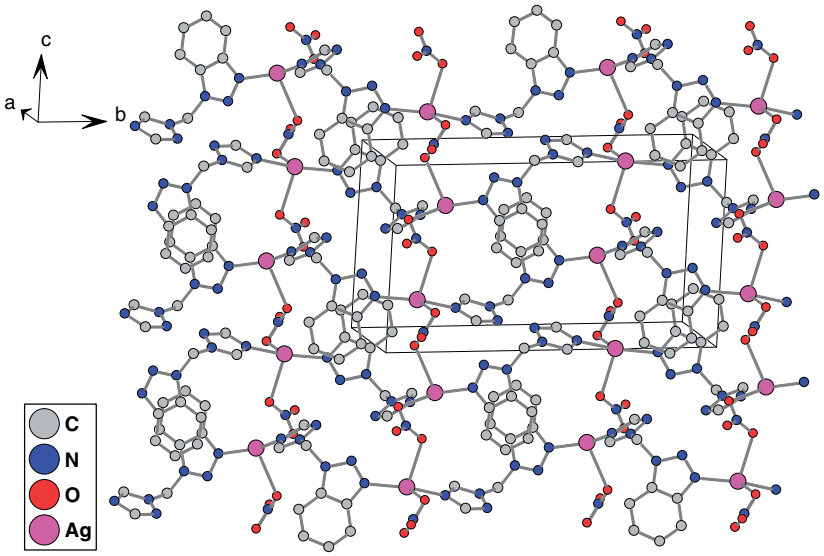

Figure 2. The two-dimensional net work of the complex **1**.

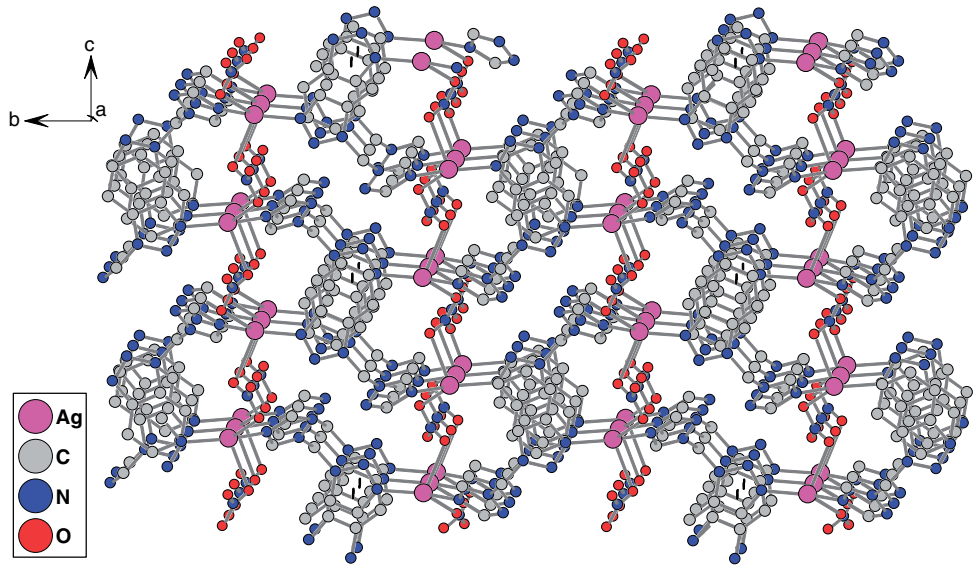

Figure 3. The three-dimensional architecture formed by $\pi - \pi$ stacking weak interactions.

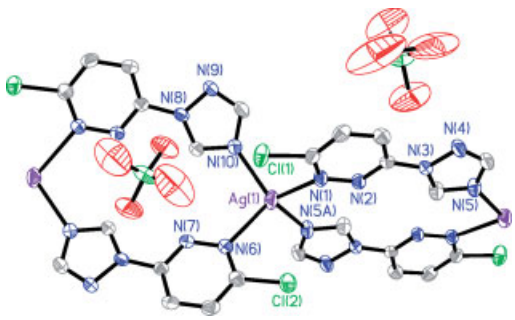

Figure 4. The molecular structure of complex **2,** and 30% probability for the ellipsoids. Hydrogen atoms are omitted for clarity.

scan technique. The structures were solved by direct methods and subsequent difference Fourier syntheses and refined on F^2 by a full-matrix least-squares method. The non-hydrogen atoms were refined anisotropically and hydrogen atoms were included in the structure factor calculation but not refined. All the calculations were carried out with the SHELX-97 and SHELXTL-97 program packages,[19] the crystal data and data collection details are summarized in Table 1.

Biological activity measurements

Measurement of fungicidal activities

The fungicidal activity of the ligands and complexes were tested *in vitro* against *Gibberalla zeae, Fusarium oxysporum, Cercospora rachidicola, Physalospora piricola* and *Alternaria solani* and their relative inhibitory ratios (%) were determined using the mycelium growth rate method.[20] After the mycelia grew completely, the diameters of the mycelia were measured and the inhibition rate was calculated according to the formula:

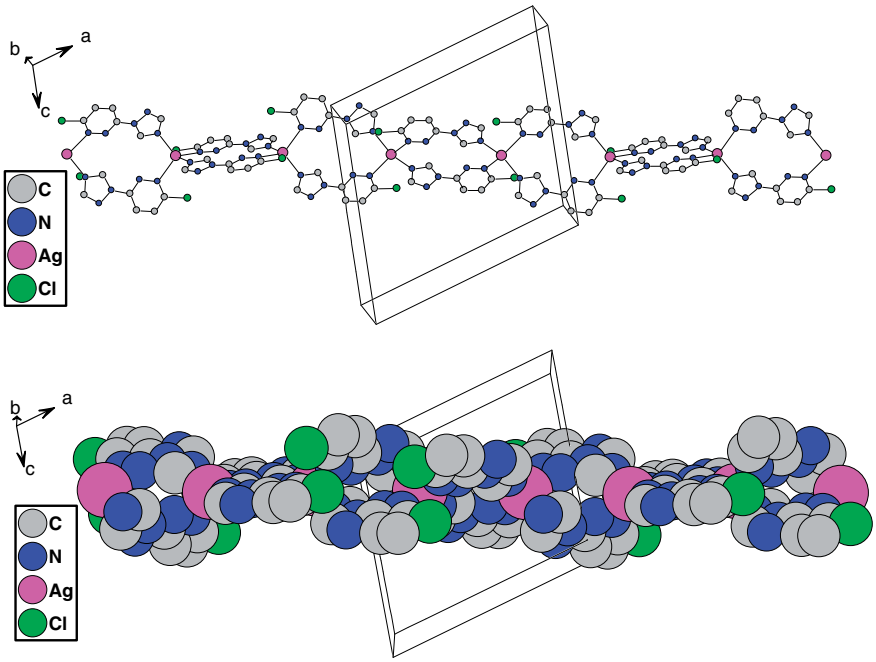

Figure 5. The flax-rope-like one-dimensional structure of complex **2**.

Table 3. Selected bonds lengths (Å) and angles (deg) for **2**

Bonds lengths			
Ag(1)–N(5)$^{\#1}$	2.238(5)	Cl(3)–O(2)$^{\#2}$	1.370(9)
Ag(1)–N(10)	2.258(5)	Cl(3)–O(1)$^{\#2}$	1.389(5)
Ag(1)–N(6)	2.443(5)	Cl(4)–O(4)$^{\#3}$	1.290(10)
Ag(1)–N(1)	2.496(5)	Cl(4)–O(3)$^{\#3}$	1.342(7)
N(5)–Ag(1)$^{\#1}$	2.238(5)	N(8)–C(10)$^{\#2}$	1.420(7)
C(10)–N(8)$^{\#2}$	1.420(7)	O(4)–O(4)$^{\#3}$	1.70(3)
Bonds angles			
N(5)$^{\#1}$–Ag(1)–N(10)	133.7(2)	O(1)–Cl(3)–O(1)$^{\#2}$	111.2(6)
N(5)$^{\#1}$–Ag(1)–N(6)	108.86(18)	O(4)$^{\#3}$–Cl(4)–O(3)$^{\#3}$	107.4(6)
N(10)–Ag(1)–N(6)	100.68(17)	O(4)–Cl(4)–O(3)$^{\#3}$	117.4(8)
N(5)$^{\#1}$–Ag(1)–N(1)	103.17(16)	O(4)$^{\#3}$–Cl(4)–O(3)	117.4(8)
N(10)–Ag(1)–N(1)	99.35(18)	O(3)$^{\#3}$–Cl(4)–O(3)	119.3(8)
N(6)–Ag(1)–N(1)	109.49(16)	C(5)–N(5)–Ag(1)$^{\#1}$	124.3(4)
N(7)–C(10)–N(8)$^{\#2}$	112.8(5)	C(6)–N(5)–Ag(1)$^{\#1}$	132.9(4)
C(9)–C(10)–N(8)$^{\#2}$	21.7(5)	C(11)–N(8)–C(10)$^{\#2}$	129.4(5)
O(2)$^{\#2}$–Cl(3)–O(1)$^{\#2}$	108.2(5)	N(9)–N(8)–C(10)$^{\#2}$	121.1(4)
O(2)–Cl(3)–O(1)$^{\#2}$	114.3(6)	Cl(4)–O(4)–O(4)$^{\#3}$	48.7(9)

Symmetry transformations used to generate equivalent atoms: $^{\#1}$ $-x+1, -y, -z$; $^{\#2}$ $-x+2, y, -z+1/2$; $^{\#3}$ $-x+1, y, -z+1/2$.

$$I = \frac{\overline{D_1} - \overline{D_0}}{\overline{D_1}} = 100\%$$

in which I is the inhibition rate, $\overline{D}_1$ is the average diameter of mycelia in the blank test, and $\overline{D}_0$ is the average diameter of mycelia in the presence of the compounds.

Measurement of radical-scavenging activities

The radical-scavenging activities of ligands and complexes were tested using the pyrogallol autoxidation method.[21] For the control experiment, Tris-HCl buffer (5 ml, pH = 8.2) was mixed with double-distilled water (5 ml), and the mixture was kept at 25.0 ± 0.2 °C for 20 min. To the mixture, 0.3 ml of pyrogallol solution (3 mmol dm^{-3}) in HCl (0.1 mmol. dm^{-3}) was added quickly with stirring, and the solution was quickly transferred to the cell for absorption measurement at 325nm on a Shimadzu UV-2450 spectrophotometer. A plot of absorption vs time (s) gave a straight line whose slope was taken as the autoxidizing velocity of pyrogallol.

For the two ligands and two complexes, solutions of the samples at various concentrations were kept at 25.0 ± 0.2 °C for 20 min, respectively. To each solution, 0.3 ml of pyrogallol solution (3 mmol dm^{-3}) was added and the solution analyzed using the same procedures as above. Plots of the absorption data of pyrogallol at various concentrations of the four compounds vs time (seconds) were made, and the rates of oxidation of pyrogallol were obtained from the slopes of the lines.

Results and Dissusion

X-ray structural characterization

*Crystal structure of $[Ag(L_1)(NO_3)]_\infty$, **1***

An ORTEP view of **1** is shown in Fig. 1. Selected bond distances and angles are given in Table 2. From Fig. 1 it can be seen that the silver atom is in a tetrahedron environment, being coordinated by two N atoms of L_1 and two nitrate O atoms. The O(3A)–Ag bond can be considered as a semi-bond due to the longer distance [O(3A)–Ag = 2.630 Å] than normal, which is slightly longer than that of O(1)–Ag [O(1)–Ag = 2.586(5) Å]. Bond lengths of Ag–O_{NO3}^- are much longer than those of Ag–N [Ag (1)–N (6) = 2.181(4) Å, Ag (1)–N (1)$^{\#1}$ = 2.187(4) Å], which indicates that the NO_3^- group has a weaker coordination ability than that of L_1. The L_1 ligand not only coordinates with the Ag(I) center but also bridging links two Ag(I) atoms by $N_{Triazole}$ and $N_{bentriazole}$. The flexible N-1-methyl-benzotriazole group leads to

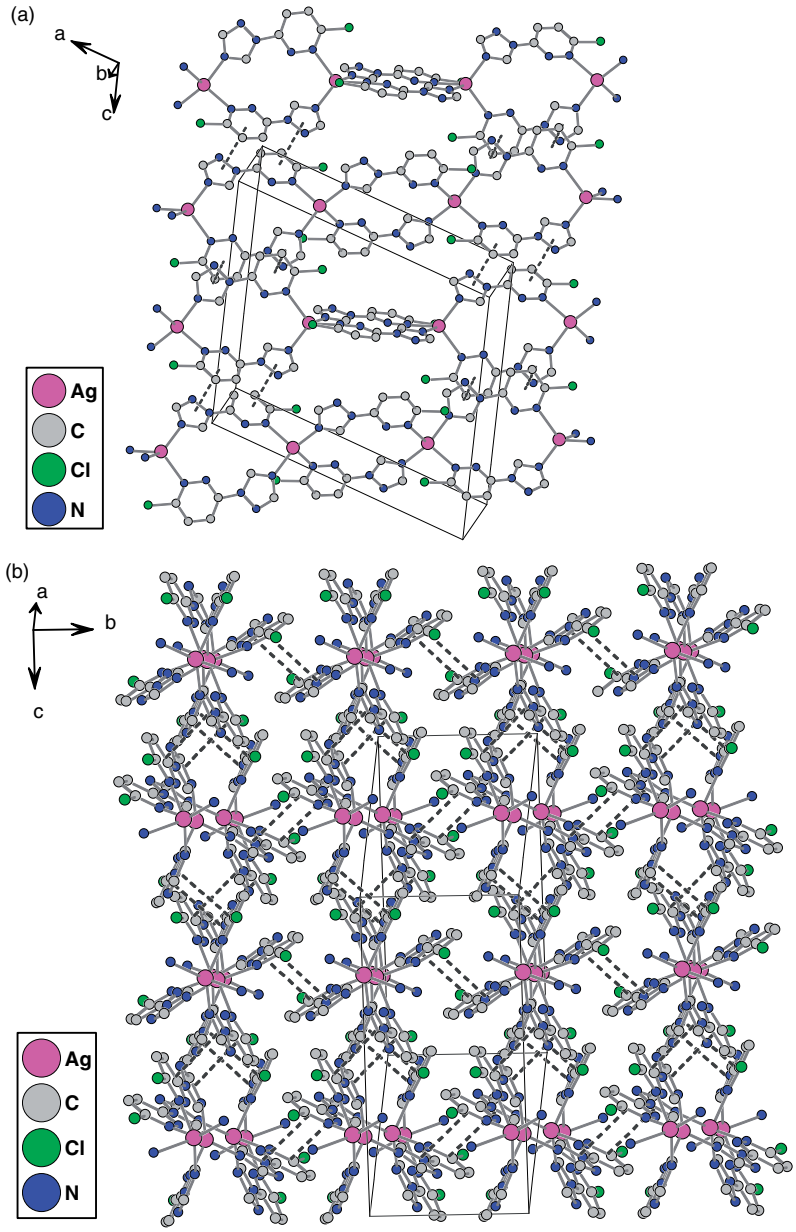

Figure 6. (a) The $\pi - \pi$ stacking weak interactions in the complex **2**. (b) The three-dimensional topological framework formed by $\pi - \pi$ stacking weak interactions.

the formation of a zigzag linear configuration in **1,** which is further linked into a two-dimensional network by coordinated NO_3^- groups. Four Ag atoms are linked by two ligands and two nitrate groups to form a 24-membered macrocycle (Fig. 2). The Ag–Ag nonbonding distance in the tetra-nuclear unit, $[Ag_4L_2(NO_3)_2]$, is 5.102 and 9.471 Å. The two-dimensional network is developed into a three-dimensional architecture through the intermolecular $\pi - \pi$ stacking weak interactions between benzene and triazole rings with the centroid–centroid separation of 3.568 Å and a dihedral angle of 1.1°, which further stabilizes the structure of **1** (Fig. 3).

Crystal structure of $[Ag(L_2)_2(ClO_4)]_\infty$, ***2***

A perspective view of **2** is given in Fig. 4. Selected bond distances and angles are summarized in Table 3. In complex **2**, the Ag(I) atom adopts a four-coordinated distorted tetrahedron geometry involving two triazole N atoms and two pyridazine N atoms of four L_2 ligands. The distances of $N_{pyridazine}$ – Ag [2.496(5) and 2.443(5) Å] are significantly longer than those of $N_{triazole}$ – Ag [2.258(5) and 2.238(5) Å], which indicates that the triazole ring has a stronger coordinated ability than that of the pyridazine ring because the electronic density on the triazole ring is higher than that on the pyridazine ring. Two Ag(I) centers are linked into a 14-member macrocycle by two rigid L_2 ligands to present a one-dimensional flax-rope-like chain (Fig. 5). The $\pi - \pi$ stacking weak interactions develop the repeat units into a three-dimensional topological framework [Fig. 6(a, b)] with the centroid–centroid distance being 3.738 and 3.681 Å, respectively, and the dihedral angle 3.67 and 3.37 deg, respectively.

From the molecular structures of two complexes, it is possible to draw the following conclusions. Firstly, the substituted groups on

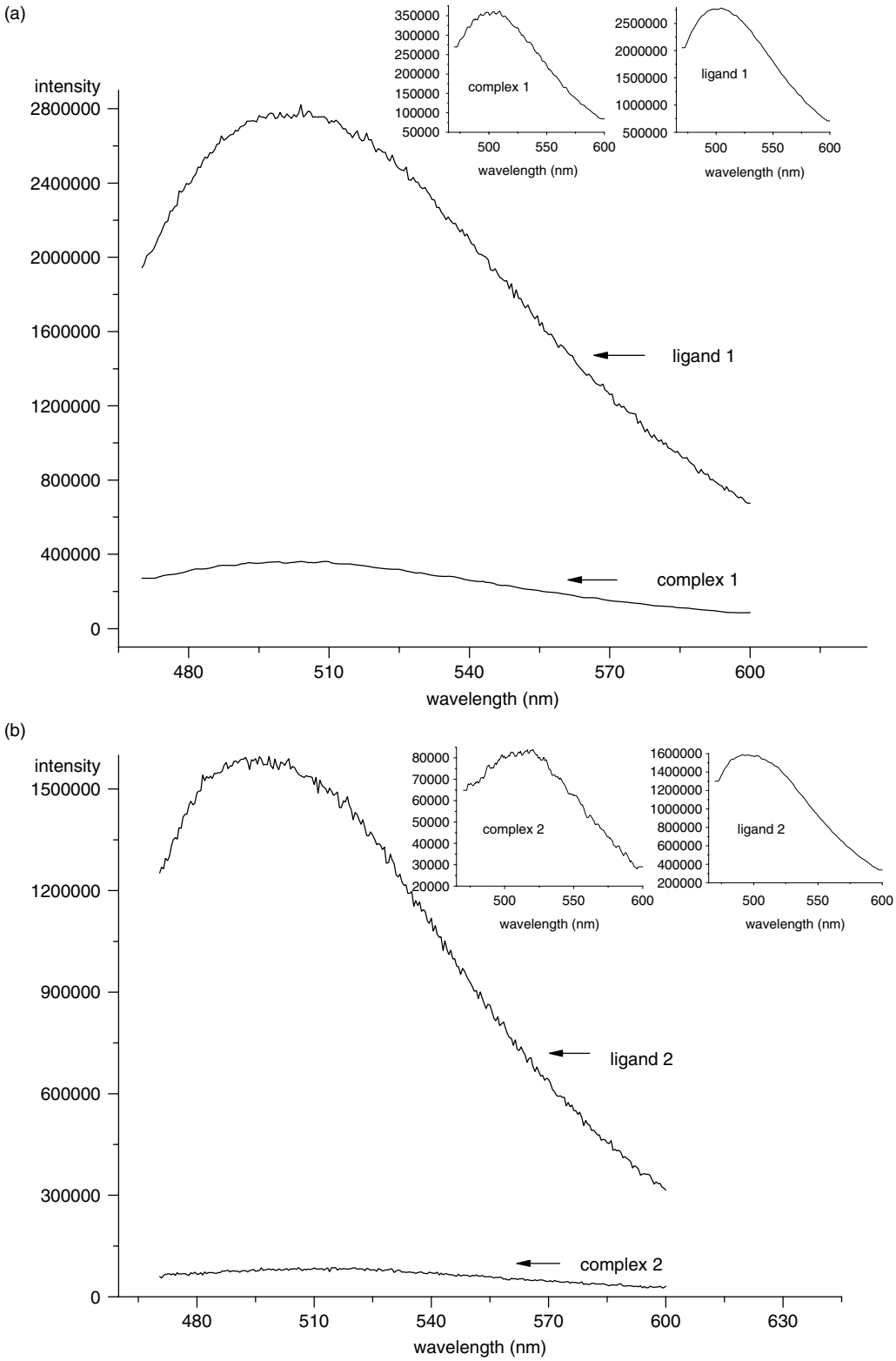

Figure 7. (a) Emission spectra of **1** and L_1 in the solid state at room temperature. (b) Emission spectra of **2** and L_2 in the solid state at room temperature.

the triazole ring affect the coordinated configuration: in complex **1**, the flexible N-1-methyl-benzotriazole group on triazole ring makes complex **1** present a two-dimensional grid-like network. However, in complex **2**, the rigid 6-chloro-pyridazine substituted group on the triazole ring makes the configuration of **2** exhibit an one-dimensional flax-rope-like chain; secondly, the coordinated counter ions stabilize the configuration of the complex: in **1**, the NO_3^- group is not only a coordination donor but also a bridging ligand, while in **2**, the ClO_4^- group only balances the electron on the compound due to its weaker coordinated ability.

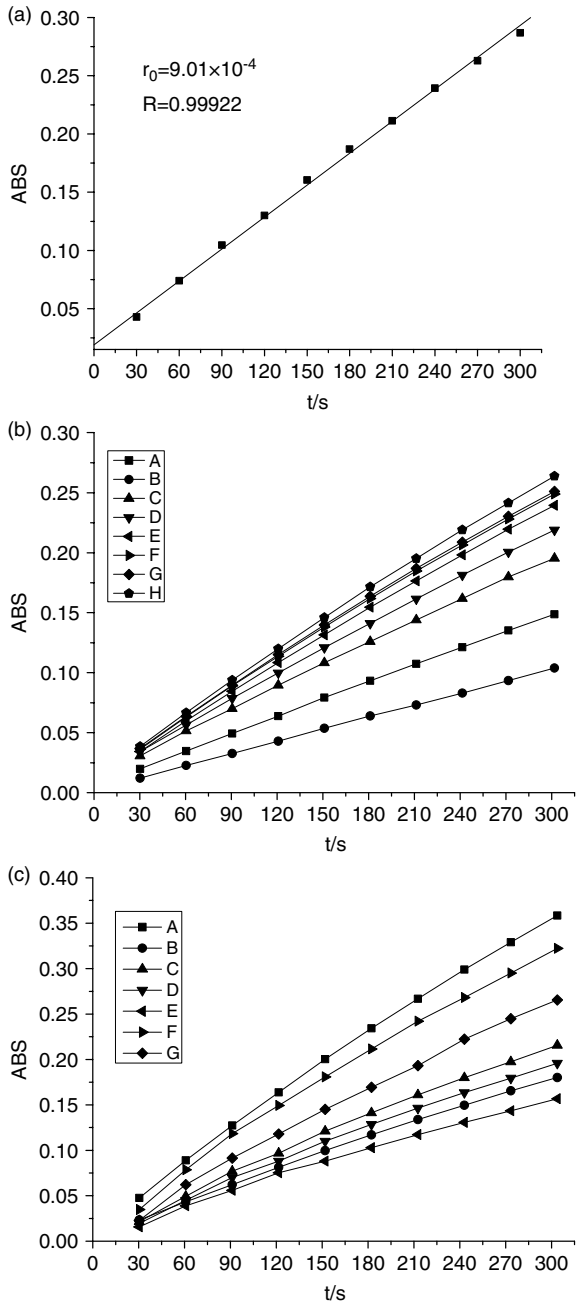

Figure 8. (a) The self-oxidazing velocity of pyrogallol. (b) Plots on the absorption (A) of pyrogallol vs time (s). The concentrations of L_1 added in samples A–G were 2, 4, 8, 12, 20, 30, 40 and 50 μg ml^{-1}, respectively. (c) The plots on the absorption (A) of pyrogallol vs time (s). The concentrations of L_2 added in samples A–G were 2, 4, 8, 12, 20, 30 and 40 μg ml^{-1}, respectively.

Luminescent properties

The luminescent properties of ligands and complexes in the solid state have been investigated at room temperature. As indicated in Fig. 7 (a, b), excitation at 445 nm leads to fluorescent emission bands at 504.5 nm for **1** and 509 nm for L_1, and 420.5 nm for **2** and 491 nm for L_2, respectively, assigned to the ligands–metal charge transfer (LMCT).The emission bands of complexes **1** and **2** exhibit certain blue-shifts compared with the corresponding free ligand. The emission strengths of the metal complexes are much weaker than those of the corresponding ligands due to the formation of the coordination metal–N bonds, which indicate that the fluorescent emissions of both complexes are ligand-based emissions.

Table 4. Fungicidal activity of the ligands and their metal complexes

	Relative inhibitory ratio (%)[a]				
Compound	Gibberalla zeae	Fusarium oxysporum	Cercospora rachidicola	Physalo-spora piricola	Alter-naria solani
L1	17.9	35.7	26.8	62.4	56.9
1	59.7	53.6	39.0	86.1	72.5
$AgNO_3$	56.3	88.9	70.0	88.0	87.5
L2	0	13.2	0	33.9	7.1
2	31.3	20.8	22.7	73.1	57.9
$AgClO_4$	62.5	88.9	90.0	92.00	87.5

[a] The data are the averages of three tested results.

Table 5. The effect of L_1 and L_2 on the autoxidation of pyrogallol

L_1 concentration (μg ml^{-1})	r_i (10^{-4})	η (%)	L_2 concentration (μg ml^{-1})	r_i (10^{-4})	η (%)
2	8.3	7.38	2	11.7	0.847
4	7.9	11.9	4	11.2	5.084
8	7.8	12.7	8	9.59	18.73
12	7.6	15.7	12	8.72	26.10
20	6.8	24.0	20	6.91	41.44
30	6.1	32.2	30	6.25	47.03
40	4.8	46.9	40	4.12	65.08
50	3.4	62.5	50	–	–

Biological activities

Fungicidal activity

The inhibition ratio of the ligands and their complexes at 50 μg cm^{-3} has been determined, and the results are summarized in Table 4. The activities of $AgNO_3$ and $AgClO_4$ have been measured at the same condition and added for comparing. From the data, it can be seen that: (1) both Ag complexes exhibit better activities than those of the ligands, the main reason being the biological activity of the silver ion; (2) the molecular structure of L_1 ligand involves both triazole and bentriazole, but L_2 ligand has only triazole, and the activity of **1** is better than that of **2** because L_1 has higher activity than that of L_2, which indicates that the more azole rings in the compounds, the higher antibacterial activity; and (3) the activities of both complexes are lower than those of the simple inorganic salts, the main reason might be that too many holes in the coordination polymers become a refuge for bacteria, decreasing the activity of the polymers. The relationship of the configuration of the complex with fungicidal activity is not clear.

Radical-scavenging activities

The autoxidizing velocity of pyrogallol, γ_0, and the autoxidation of pyrogallol after adding L1 and L2 at various concentrations was obtained from plots of absorption vs time, as shown in

Fig. 8(a–c), respectively. The autoxidizing velocities of pyrogallol at various concentrations of L, γ_i, are summarized in Table 5. It is found that the greater the concentration of L, the lower the velocity of pyrogallol autoxidation. The IC_{50} value of L_1 and L_2 is 4.52 and 32.76 μg ml^{-1}, respectively, which indicates that the L_1 and L_2 have certain radical-scavenging activities. The inhibition rate (η) is calculated by the formula: $\eta = [1 - (\gamma_i/\gamma_0)] \times 100\%$. The radical-scavenging activities of the metal complexes **1** and **2** are not obvious (Table S1 and S2), which might be due to the generation of some color species from the oxidation, interrupting the pyrogallol autoxidation.[22]

Supporting information

Supporting information can be found with the online version of this article. The crystallographic data for structural analysis of two metal complexes have been deposited with the Cambridge Crystallographic data centre, nos CCDC 665811 for **1** and CCDC 665812 for **2**.

References

[1] F. X. Tavares, J. A. Boucheron, S. H. Dickerson, *J. Med. Chem.* **2004**, *47*(19), 4716.
[2] B. E. A. Steck, R. Bruline, L. T. Fletcher, *J. Am. Chem. Soc* **1954**, *76*, 4454.
[3] S. Julia, P. Sala, J. D. Mazo, M. Sancho, C. Ochoa, J. Elguero, J. P. Fayet, M. C. Vertut, *J. Heterocycl. Chem.* **1982**, *19*, 1141.
[4] S. Julia, J. D. Mazo, L. Avila, J. Elguero, *Org. Prep. Proc. Int.* **1984**, *16*, 299.
[5] J. Torres, J. L. Lavandera, P. Cabildo, R. M. Claramunt, J. Elguero, *J. Heterocycl. Chem.* **1988**, *25*, 771.
[6] G. G. Lobbia, F. Bonati, A. Cingolani, D. Leonesi, A. Lorenzotti, *Synth. React. Inorg. Met. Org. Chem.* **1988**, *18*, 535.
[7] G. G. Lobbia, F. Bonati, *Synth. React. Inorg. Met. Org. Chem.* **1988**, *18*, 551.
[8] S. K. Mandal, L. K. Thomopson, E. Gabe, *J. Inorg. Chem.* **1987**, *27*, 855.
[9] G. A. Ardizzoia, S. Cenini, G. L. Monica, *Inorg. Chem.* **1994**, *33*, 1458.
[10] J. G. Haasnoot, *Coord. Chem. Rev.* **2000**, *200*, 131.
[11] S. Trofimenko, *J. Am. Chem. Soc.* **1967**, *89*, 3170.
[12] J. G. Haasnoot, *Coord. Chem. Rev* **2000**, *200*, 135.
[13] L. F. Tang, Z. H. Wang, J. F. Chai, X. B. Leng, J. T. Wang, H. G. Wang, *Polyhedron* **2000**, *19*, 1949.
[14] F. Effendy, C. Marchetti, R. Pettinari, B. W. Skelton, A. H. White, *Inorg. Chem.* **2003**, *42*, 112.
[15] L. F. Tang, Z. H. Tang, J. F. Chai, X. B. Leng, J. T. Wang, H. G. Wang, *J. Organomet. Chem.* **2002**, *642*, 179.
[16] Y. Carcia, PJvan Koningsbruggen, H. Kooijman, A. L. Spek, J. G. Haasnoot, O. Kahn, *Eur. J. Inorg. Chem.* **2000**, 307.
[17] A. R. Kartrizky, M. D. Deyrup, X. F. Lan, F. Brunner, *J. Heter. Chem.* **1989**, *26*, 829.
[18] C. C. Tang, Y. C. Li, B. Chen, *Pesticide Chemistry*. Nankai University Press: Tianjin, **1998**.
[19] G. M. Sheldrick, *SHELXS-97, Acta Crystallogr.* **1990**, *A46*, 467; b) G. M. Sheldrick, *SHELXL-97, Program for X-ray Crystal Structure Refinement*, University of Göbttingen: **1997**.
[20] N. C. Chen, *Bioassay of Pesticides*. Beijing Agricultural University Press: Beijing, **1991**, p. 161.
[21] R. K. Castellano, F. Diederich, E. A. Meyer, *Angew. Chem. Int. Edn* **2003**, *42*(11), 1210.
[22] S. Marklund, G. Marklund, *Eur. J. Biochem.* **1974**, *47*, 469.

